H.R. Guzmán-Carrillo, J.M. Pérez, M. Romero, Coal fly ash and steel slag valorisation throughout a vitrification process. *International Journal of Environmental Science and Technology 15 (2018) 1757-1766;* doi: 10.1007/s13762-017-1542-5

Coal fly ash and steel slag valorisation throughout a vitrification process.

HR Guzmán-Carrillo [1, *], JM Pérez [2], EA Aguilar Reyes [1], M Romero [2, **]

[1] Instituto de Investigación en Metalurgia y Materiales, Universidad Michoacana de San Nicolás de Hidalgo, Ciudad Universitaria Morelia, 58030, Michoacán, México

[2] Grupo de Materiales de Vidrio y Cerámica, Instituto Eduardo Torroja de Ciencias de la Construcción, CSIC, C / Serrano Galvache 4, 28033, Madrid, España

[*] Dirección actual: CINVESTAV, IPN Unidad Querétaro, 76230, Querétaro, México

[**] Correo electrónico del autor correspondiente: mromero@ietcc.csic.es

Abstract

The aim of this research was to evaluate the feasibility of using the vitrification process as an alternative solution to the disposal of a coal fly ash and metallurgical slags in landfills. The starting wastes were characterised in terms of chemical, granulometric, mineralogical, and microstructural analysis. A selected batch composition composed by 58.5% fly ash, 31.5% metallurgical slag and 10.0 Na_2O% (weight percentage) were melted at 1450 °C and poured to obtain monolithic glass samples. The environmental behaviour of the starting wastes and the resulting glass was evaluated by standard leaching tests, which shows that vitrification leads to a stabilization process in which the inorganic components of the wastes are immobilized throughout their incorporation into the glass structure. Moreover, vitrification transforms those hazardous wastes into a new non-hazardous glass. A preliminary study shows that the new glass is suitable for developing glass-ceramic tiles appropriate for floor pavement and wall covering.

Keywords: Waste disposal; Recycling; Leaching test; Glass; Glass-ceramics

1. Introduction

Since the late nineteenth century, coal has been used as a power source. The demand for energy resources required by the world population in recent decades has lead to increased coal consumption over this period and it is expected to continue increasing. In 2011, coal-fired generation accounted for 29.9% of the world electricity supply, and its share is anticipated to be 46% by 2030 (Yao et al. 2015).

Coal fly ash is a by-product of coal combustion in thermal power plants. It accounts for 5–20 wt. % of feed coal and is normally found in the form of coarse bottom ash and fine fly ash. Coal includes considerable amount of trace metals, and after combustion these metal concentrations in fly ash are sometimes 4–10 times higher than those in parent coal. Most fly ash are deposited in open dumps without any pre-treatment, which involves a high risk of ecosystem pollution with danger to both human health and the environment.

According to the ASTM678 classification, there are two types of fly ash, namely type F and type C. The former is characterized by a high percentage of silica and alumina (70 wt% min), while Class C has a high lime percentage (20 wt% max). Both its physical and chemical properties depend on the type of coal used and combustion conditions. Fly ash have a wide range of particle size comprising between 1 and 100 microns (Erol et al. 2000) and its chemical composition consisting mainly of oxides such as silica, alumina, calcium oxide, iron oxide and some alkali oxides (Iyer and Scott 2001).

Recently, some studies analysed the concentration of heavy metals in fly ashes to access their leaching characteristics in presence of some selective low-cost additives to inhibit the degree of contamination of these heavy metals (Pani et al. 2016). Significant efforts have been also undertaken in recent years focused on the valorisation of fly ashes (Jayaranjan et al. 2014). About 20% of the fly ash generated is being used in concrete production (Faleschini et al. 2015; Pérez et al. 2014). Other uses include road base construction, soil amelioration and mine reclamation (Ram and Masto 2010; Skousen et al. 2012; Ram and Masto 2014) adsorbents for mercury removal, CO_2 capture and wastewater treatment (Zheng et al. 2012; Wee 2013); zeolite synthesis, and use as a filler in polymers. However, these applications are not sufficient for the complete utilization of the fly ash generated worldwide. Hence, a viable option for the reuse of large amounts of fly ash is vitrification. Vitrification is a process through which a material is converted into an amorphous solid free from crystalline structure (M. Romero et al. 2008). Vitrification is generally accomplished

by heating the substances until they become a melt, which is then rapidly cooled so that it passes through the Tg interval without any crystallization occurring and as result, an amorphous solid is formed.

Metallurgical slags are produced in a very large amount in pyrometallurgical processes, and are huge sources of waste if not properly recycled and utilized. Steel slag is a by-product of the steelmaking from iron with a wide range of chemical and mineral compositions, resulted by different feeding material and smelting conditions. They are produced from an oxidation process, thus have higher iron oxides contents. Moreover, alumina, calcium, magnesium and sodium oxides are major constituents. Similarly to coal fly ash, steel slags are stored or used for land filling, which has become a significant source of pollution of air, water and soil. Due to the large slag quantities and the stricter environmental regulations, re-utilization of these slags are an attractive alternative in order to reduce and eventually to eliminate the disposal cost, to minimize the related environmental pollution, and to save the resource conservation (Reuter et al. 2004).

Recent studies have revealed the feasibility of industrial and mining wastes valorisation throughout the fabrication of construction materials such as cement and mortars (Sharma and Joshi 2016; Seyyedalipour et al. 2015; Jarosz-Krzeminska et al. 2015; López et al. 2015; Gallardo et al. 2014; Saikia et al. 2015), ceramics (Verbinnen et al. 2015), clay bricks (Martínez et al. 2016; Eliche-Quesada et al. 2015) and glass-ceramics (Pan et al. 2015; Karamanov et al., 2014; Ljatifi et al, 2015). On one hand, construction ceramic materials present a high demand for global consumption, so that they can incorporate large amounts of waste in their production process. Additionally, building ceramic are fabricated from mixtures of different raw materials, namely plasticizers, fluxes, fillers, etc.; consequently, any residue is likely to become part of the composition of a ceramic body. Finally, building ceramics shows a heterogeneous microstructure; thus slight changes in the waste composition. These features have promoted different investigation aimed to produce glass, glass–ceramic and sintered materials from coal fly ash (Wang et al. 2014).

The aim of the present work was to find a friendly alternative solution to the disposal of a Mexican coal fly ash and metallurgical slags in landfills. As it was necessary to mix the fly ash with a fluxing raw material in order to obtain a workable molten, a metallurgical slag was used for adjusting the glass batch composition. This research is part of a larger study that explores the possibility of valorising Mexican coal fly ash as glass-ceramic tiles suitable for floor pavement and wall

recovering. This study was carried between 2012 and 2015 at the Eduardo Torroja Institute for Construction Sciences, Madrid, Spain.

2. Materials and Methods

2.1 Starting materials

Two different wastes were used in the glass formulation, viz., fly ash and metallurgical slag. Moreover, Na_2CO_3 was added to the glass composition to assist the melting process.

The fly ash used in this investigation was originated from Petacalco coal-fired power plant, located in La Unión, Guerrero State, Mexico. For its characterization and subsequent incorporation into the glass composition, the ash was used as-received without any prior conditioning stage. The metallurgical slag proceeds from ArcelorMittal steelmaking plant located in Lázaro Cárdenas, Michoacan State, Mexico. In this case, prior to its use, the slag was grinded by high energy milling and sieved to a particle size < 100 μm.

2.2 Materials characterization

The chemical composition of coal fly ash, steel slag and the glass developed in this study was determined by X-ray fluorescence (XRF) (Bruker model S8 Tiger equipped with the software package SPECTRA^{Plus}).

The evaluation of the crystalline nature of wastes and the developed glass was performed by X-ray diffraction (XRD) (Bruker model D8 Advance) with Ni-filtered Cu Kα radiation operating at 30 mA and 40 kV. Data were recorded in the 5-60° 2θ range (step size 0.019732º and 0.5 s counting time for each step). Crystalline phases were identified by their characteristic interplanar spacings and corresponding relative intensities by means of the Powder Diffraction File (PDF) from the International Centre for Standard Data (ICSD).

The particle size of the fly ash was determined in a laser diffraction particle size analyzer (Beckman-Coulter model LS100 Q) with a measuring range of 0.3 -1000 μm and reliability of 1%. To evaluate the thermal behaviour wastes, differential scanning calorimetry (DSC) was performed using a Setaram (Labsys) TG-DTA/DSC unit in air atmosphere. The analyses were carried out at a heating rate of 50°C/min, in platinum crucibles and calcined alumina as reference.

The microstructural analysis of wastes was performed by field emission scanning electron microscopy (FE-SEM) (Hitachi model S-4800) using an accelerate voltage of 20kV. Semi-quantitative analysis of different phases were obtained by energy dispersive X-ray spectroscopy (EDS) (Bruker model QUANTAX Esprit 1.9) provided by a beryllium (Be) window. SEM observations were performed on powder samples deposited on conducting carbon tape. The samples were Au-Pd coated in a Balzers SCD 050 sputter. The distribution of ions among the different phases was determined by digital X-ray mapping, which is an imaging technique used to analyse the two-dimensional distribution of elements in a specimen. Each two-dimensional map represents a single element and the colour variations on the map represent differences in the weight percent of the elements from point to point.

The theoretical melting temperature of the coal fly ash, steel slag and raw materials mixtures was determined by the equation proposed by Rodríguez (Rodríguez 1984):

$$T log\ \eta = \frac{\sum c_i p_i}{P_{SiO_2}} \qquad [1]$$

where $T\ log\ \eta$ is the temperature corresponding to the viscosity defined by $log\ \eta$, p_i is the concentration (wt. %) of each of the glass components, c_i is a coefficients for each of the oxides corresponding to the viscosity defined by $log\ \eta$ and P_{SiO2} is the concentration (wt. %) of SiO_2 in the composition. For applying the equation and determine the theoretical melting temperature, it was considered that the viscosity of the melt at its melting temperature has a fixed value of $10^{2.0}$ dPa s.

The environmental behaviour of the studied wastes was evaluated by one-step batch leaching tests in which a fixed amount of material is leached with a fixed amount of leachate. Tests were carried out at a liquid to solid ratio of 2 l/kg (UNE EN 12457-1) and 10 l/kg (UNE EN 12457-2), which simulate the disposal of the waste in closed and open dump sites, respectively. To perform the test, 175 g of dry waste was placed in a glass container. After adding the corresponding amount of leachant, the capped container was placed on a stirring device. The ambient temperature was maintained at 20°C for the entire test. After 24 hours of stirring, the solids in suspension were allowed to settle for 15 min. After that, the leachates were filtered over a 0.45 μm membrane filter with a vacuum filtration device. The conductivity and pH of the leachates were measured immediately. According to the Landfill of Waste Directive 2003/33/CE (OJEC, 2003), the criteria for waste acceptable at landfills for inert waste are determined by the As, Ba, Cd, Cr, Cu, Hg, Mo, Ni, Pb, Sb, Se and Zn concentrations in the leachates, which were determined by ICP (Varian 725-

ES). Ion chromatography (Metrohm 92 Basic) has been used to analyse the concentrations of F^-, Cl^- and SO^{2-}.

2.3 Wastes vitrification

After assessing the theoretical melting temperatures of fly ash and metallurgical slag, a similar estimation was performed for different ash/slag rates in order to obtain a mixture of wastes with a theoretical melting temperature within the melting range of conventional glasses (1400-1450°C).

The components of the selected batch compositions were mixed for 15 minutes in a blender (TURBULA) to get a homogeneous mixture. The batch was placed in aluminosilicate crucibles and heated at 15ºC/min in an electric furnace up to 1450°C. After a holding time of 60 minutes at the melting temperature, monolithic glass samples were made by pouring the melt into brass moulds. The environmental behaviour of the glass was evaluated by the above described UNE EN 12457-1 and 2 leaching tests.

3. Results and Discussion

3.1. Raw materials characterization

Table 1collects the chemical composition of the as-received fly ash determined by XRF. It is noteworthy that the percentage of silica and alumina is very high, about 80 wt. %. Therefore, it is an F type fly ash, which is expected to present a highly refractory behaviour in the melting process. Furthermore, the alkaline and alkaline-earth oxides content (MgO, CaO, Na_2O, K_2O and BaO) is very low (< 4 wt. %). Namely, it is devoid of modifiers network elements which are necessary for the easy formation of a glass.

Table 1. XRF analysis (wt %) of the as-received Petacalco coal fly ash.

SiO_2	Al_2O_3	Fe_2O_3	MgO	CaO	Na_2O	K_2O	SO_3	P_2O_5	TiO_2
56.05	23.37	7.24	0.83	2.29	0.47	1.31	1.41	0.29	1.22

Figure 1a shows the XRD pattern of the fly ash. The main crystalline phases are α-quartz (SiO_2), hematite (Fe_2O_3) and mullite ($Al_6Si_2O_{13}$). However, the diffractogram displays a notable hallo in the 18 <2θ> 29 interval, which indicates the occurrence of a significant amount of amorphous phase.

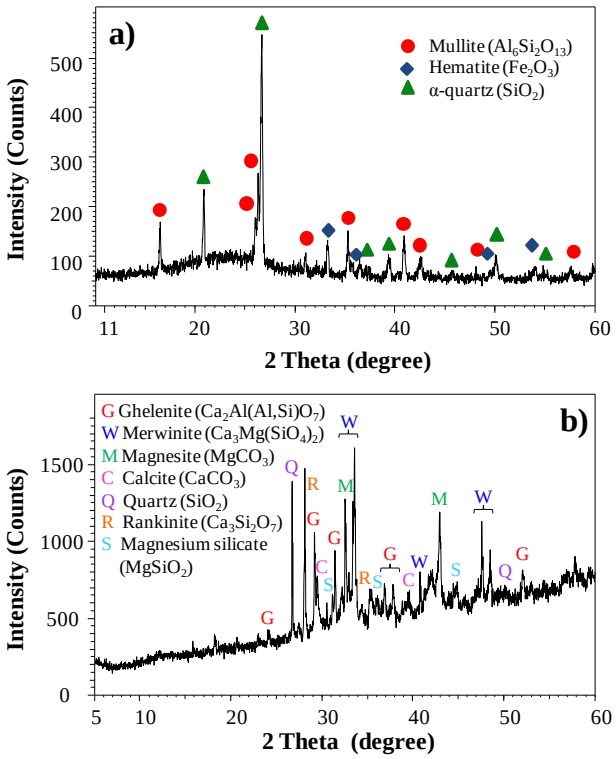

Fig. 1 X-ray diffraction pattern of a) the as-received Petacalco coal fly ash and b) Arcelor Mittal metallurgical slag sieved to a particle size < 100 µm

Figure 2 presents the cumulative particle size distribution of the fly ash. It is noted that the ash shows a very fine particle size, including in a wide range, namely from 0.3 to 161.2 µm, with values of D_{50} and D_{80} equal to 37.65 microns and 76.13 µm, respectively.

According to Fernández Navarro (2003), particle size is one of the determining factors for the use of sand in the production of glass. For melting in crucible, it is considered an optimum particle size in the 0.1 and 0.3 mm range. The proportion of fines with size lower than 0.1 mm should be insignificant, usually a lesser amount of 1%, since fine grains react too fast and promotes the development of a highly viscous melt, which would require a longer refining time. Moreover, the

specific surface increases as the proportion of fines decreases. A larger specific surface promotes a higher reaction speed on the first melting steps and consequently, the viscosity of the melt increases. According to this criterion, the particle size of Petacalco fly ash is too fine, with about 90% of the sample with particle size lower than 100 µm. Therefore, it is expected that the vitrification of this ash leads to a high viscosity melt, requiring the addition of fluxing elements to improve its workability.

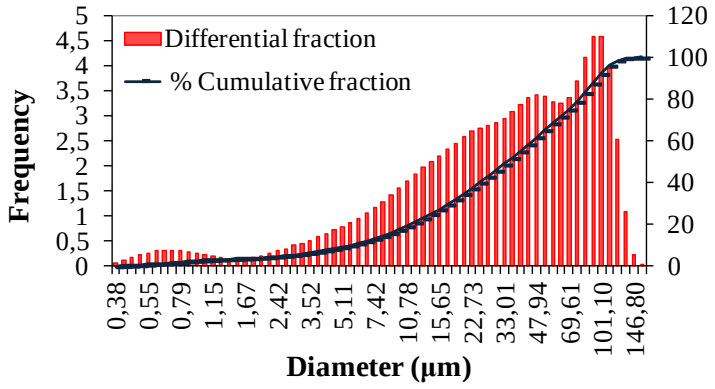

Fig. 2 Cumulative distribution and particle size frequency curves of the as-received Petacalco fly ash

Figure 3 shows the microstructure of the Petacalco fly ash observed by FE-SEM. As usual in coal fly ashes (Fomenko et al. 2013), the microstructure is mainly comprised of spherical particles (cenospheres) having a wide range of particle size, with diameter ranging from a few microns to about 120 microns (Fig. 3a), which agrees with the particle size distribution (Fig. 2). The analysis by digital X-ray mapping reveals the distribution of ions among the different particles. Thus, Fig 3b shows a FE-SEM image together with the elemental mapping of Si, Al, C, Fe and Ca. The EDS analyses of the different particles are collected in Table 2. The chemical composition of different particles showed in Table 2 corresponds to the average composition determined from the EDS analyzes performed on 20 different particles. The major chemical components of cenospheres are silicon and aluminium. A smaller amount of cenospheres are enriched in iron due to the concentration of hematite crystals therein. Fig. 3c shows an iron-rich sphere together with its EDS spectrum (Fig. 3d) showing the high intensity of the Fe lines. Moreover, agglomerates or unburned

carbon particles are clearly identified by colour dissimilarities and EDS analyses (Fig 3e). Finally, calcium-rich agglomerates are also found dispersed in the whole fly ash sample.

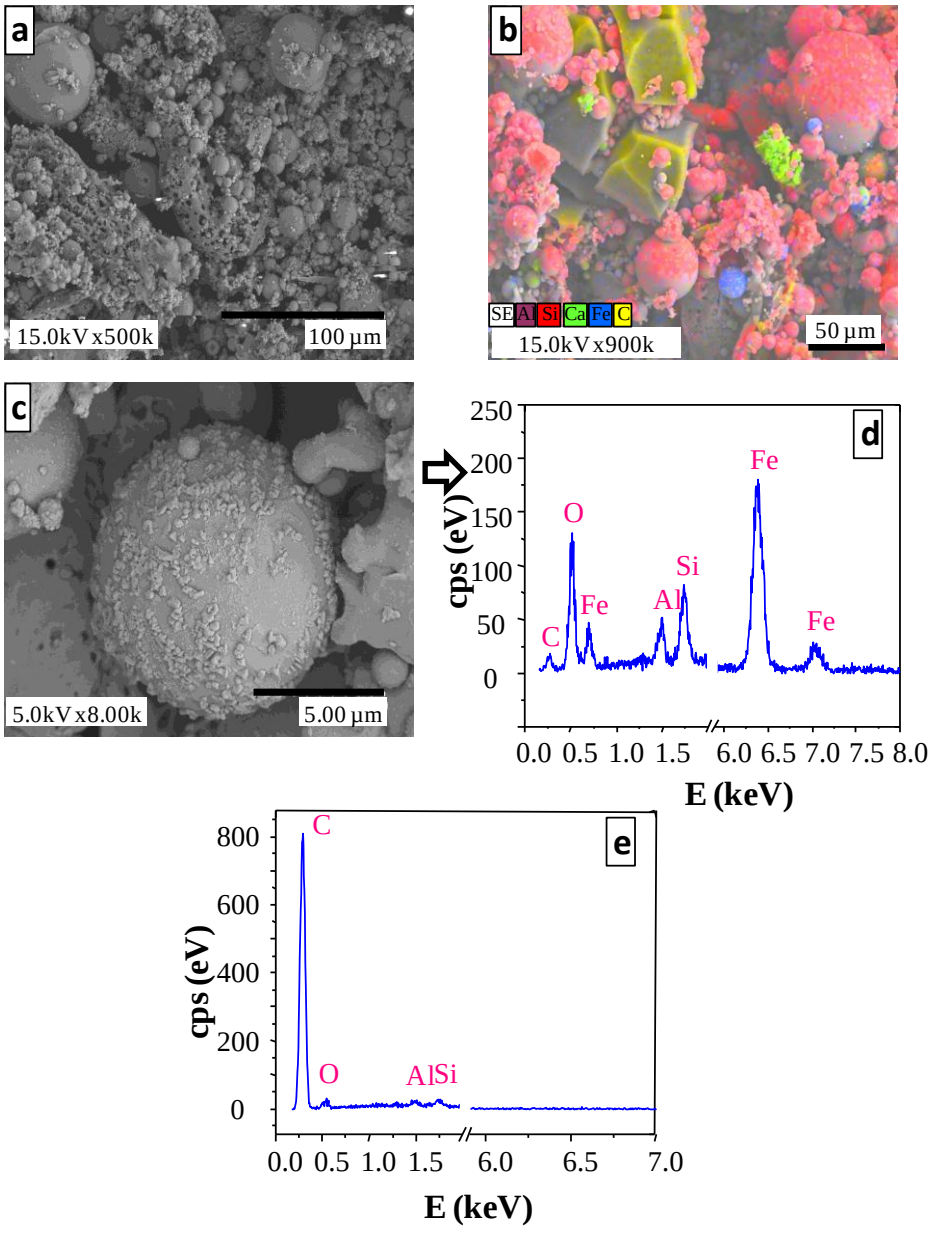

Fig. 3 Microstructural FE-SEM analysis of Petacalco fly-ash a) general view of cenospheres; b) X-ray mapping; c) microstructure of an iron-rich sphere; d) EDS spectrum of an iron-rich sphere; e) EDS spectrum of unburned carbon particles

Table 2. EDS analyses (wt %) collected on different particles making up the Petacalco fly ash.

	Cenospheres	**Iron-rich cenospheres**	**Calcium-rich agglomerates**
Na	0.37±0.07	---	0.24±0.02
Mg	0.43±0.03	---	0.07±0.01
Al	10.13±2.94	2.61±0.35	5.38±0.6
Si	33.50±0.45	4.98±0.28	3.52±0.23
P	0.43±0.06	0.30±0.03	0.32±0.05
K	2.81±0.20	0.05±0.01	0.56±0.06
Ca	0.54±0.03	0.09±0.02	56.42±2.39
Ti	0.29±0.02	0.25±0.08	0.14±0.06
Fe	1.82±0.32	64.61±0.16	0.98±0.18
O	49.69±1.51	27.11±1.18	32.37±0.63

Figure 4a shows the DSC/TG curve of the fly ash. The initial 2.2 % weight loss up to 320°C corresponds to the release of water adsorbed in the surface of fly ash particles. After that, a weight reduction of 6.4% in the range 460º-950ºC is associated to the thermal dissociation of residual carbon, which can be also detected in the DSC curve by a broad exothermic peak with a non-defined shape, as it includes several shoulders due to the overlapping of the different reactions comprised in the oxidation reaction of unburned carbon. A similar behaviour was previously reported in the thermal characterisation of coal fly ashes (Kim and Kim 2004). It is important to

note that neither endothermic peaks nor variation of TG curve, indicative of the formation of liquid phases are observed at high temperature. Therefore, it is expected that the fly ash show a refractory behaviour. In fact, the theoretical melting temperature of the fly ash, calculated according to Eq. [1] is 1758ºC. Consequently, obtaining a glass will require mixing with a raw material enriched in fluxing elements (alkaline or alkaline-earth) in order to decrease the glass melting temperature. Considering the current interest in reducing the environmental impacts of waste generated by industrial activities, it was determined the use of another industrial waste to decrease the melting temperature of the glass composition and thus, a metallurgical slag was selected as fluxing raw material.

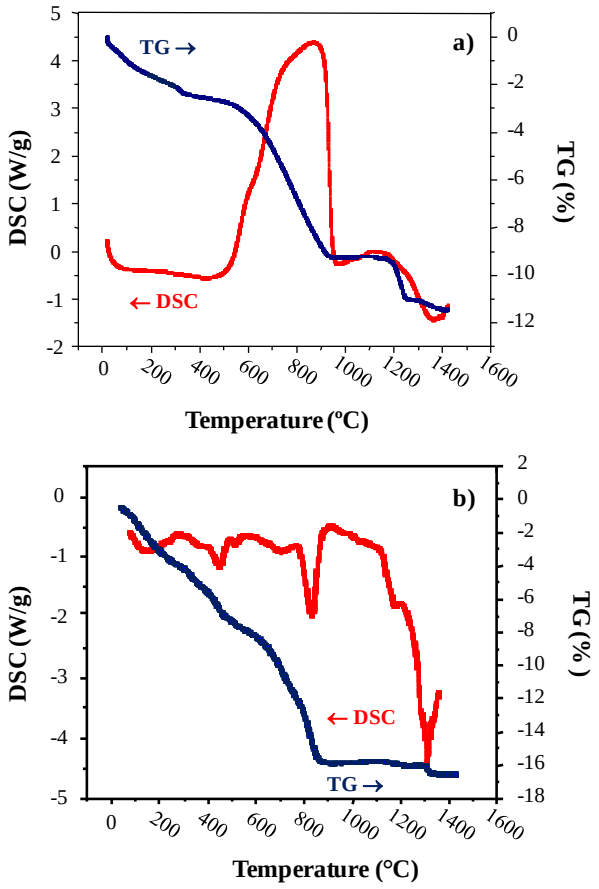

Fig. 4 DSC/TG curve of a) the as-received Petacalco fly ash and b) Arcelor Mittal metallurgical slag sieved to a particle size < 100 µm

Table 3 and Figure 1b show the chemical composition determined by XRF and the X-ray diffraction pattern of the steel slag. The low content (~25 wt. %) in network forming elements, such as SiO_2 and Al_2O_3, along with its high percentage in alkaline and alkaline-earth elements (~60 wt. %), makes this steel slag useful for balancing out the deficit of fluxing elements in the coal fly ash. Similarly to the fly ash, the diffractogram of the slag shows a significant background, which is characteristic of materials with amorphous phase in its constitution. The main mineral phases are gehlenite ($Ca_2Al_2SiO_7$) merwinite ($Ca_3MgSi_2O_8$), magnesite ($MgCO_3$), calcite ($CaCO_3$), α-quartz (SiO_2), rankinite ($Ca_3Si_2O_7$) and magnesium silicate (Mg_2SiO_4).

Table 3. XRF analysis (wt %) of Arcelor Mittal metallurgical slag.

SiO_2	**Al_2O_3**	**Fe_2O_3**	**MgO**	**CaO**	**Na_2O**	**MnO**	**SO_3**	**P_2O_5**	**TiO_2**
17.66	6.78	6.87	12.12	42.87	3.22	1.40	1.41	0.24	0.52

Figure 5 shows the microstructure of the Arcelor Mittal metallurgical slag observed by FE-SEM. The low magnification SEM image (Fig. 5a) reveals the heterogeneity of the slag, which is made up of particles and aggregates of different size and nature as is evidenced by the X-ray mapping (Fig. 5b). However, in this case there is no possibility to confirm by EDS analysis the different crystalline phases identified in the mineralogical study (Fig. 1b) due to both the high degree of mixing of the different phases and the small size of the particles, which often is below the lateral resolution of the method of analysis (1µm). Higher magnification images (Fig. 5c,d) allow to perceive long, slender crystals with columnar habit, which is characteristic of calcite.

Figure 4b presents the DSC/TG curve for the metallurgical slag. The existence of different endothermic effects is indicative of transformation or decomposition reactions of the crystalline phases comprised in the slag. Thus, a small peak at 510°C corresponds to the quartz α→ β transformation. Moreover, the endothermic effect at 820°C is related to the dissociation of calcite. Finally, a sharp endothermic effect beginning at 1080°C which reaches a minimum at 1300°C is due to formation of liquid phases. TG analysis shows a continued weight loss of 16%, which is

associated to carbon dioxide release as consequence of carbonates decomposition. Both, the beginning of liquid phases formation by DSC and the theoretical melting temperature calculated from Eq. 1 (1064ºC) indicates that this metallurgical slag would be a appropriate raw material to add to the ash in order to obtain a melt with suitable viscosity at the melting temperature of 1450ºC.

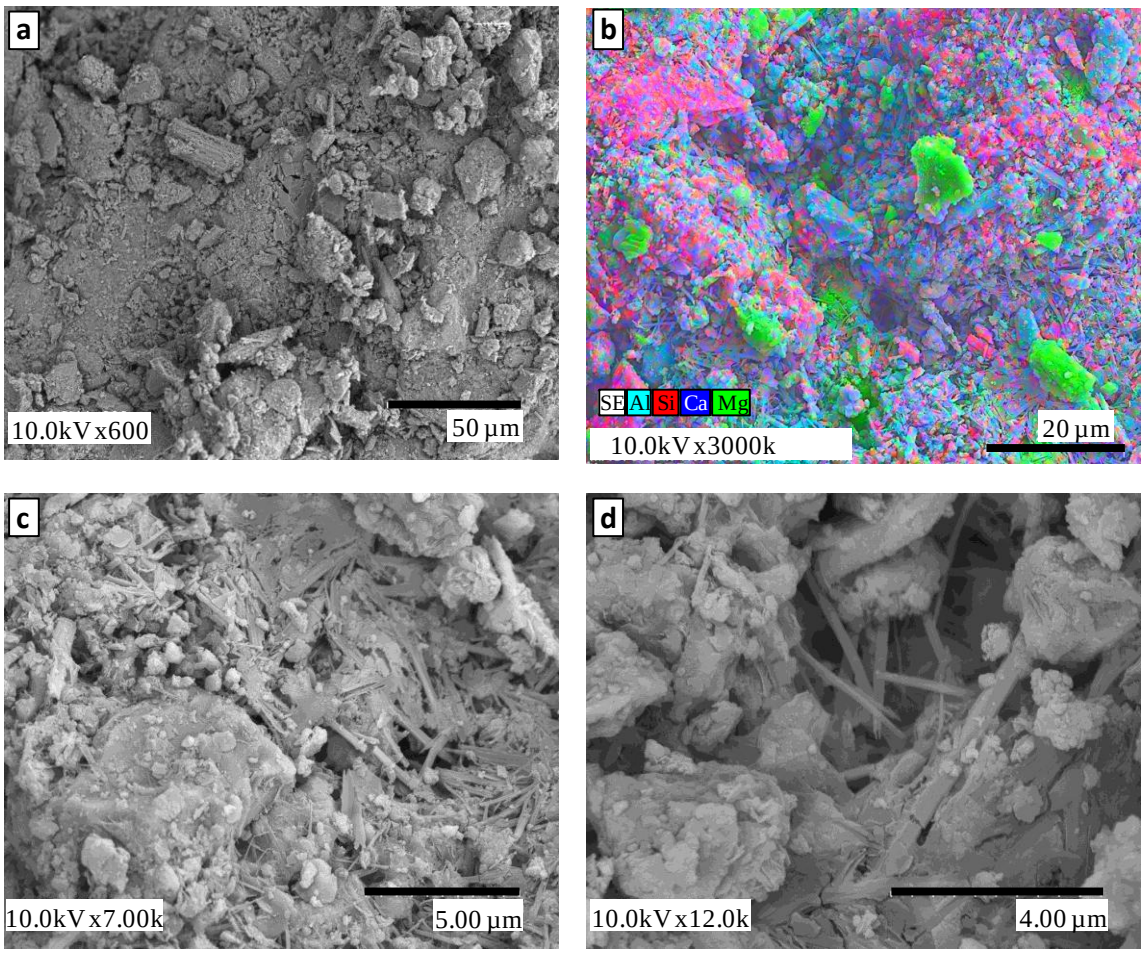

Fig. 5 Microstructural FE-SEM analysis of Arcelor Mittal metallurgical slag

3.2 Wastes vitrification

After characterizing the fly ash and the metallurgical slag, it is evident that the theoretical melting temperature of the fly ash (1758°C) is too high to vitrify without the assistance of a flux and that the metallurgical slag is a suitable complementary raw material for formulating glass compositions. It is noteworthy that the amount of fly ash in the composition should be maximized, as the recovery of this waste is the main objective of this study. After determining the theoretical melting temperature of a series of mixtures with different ash/slag ratio, the compositions 70%C30%E, 65%C35%E and 50%C50%E where C and E denotes fly ash and metallurgical slag respectively, were selected for preliminary melting tests. The theoretical melting temperatures for those compositions were 1440º, 1369º and 1292ºC respectively. The CE50-50 composition is the only having an appropriate behaviour in the melting process and leads to a melt with a proper viscosity. However, this composition is rejected considering that the percentage of ash is low. Therefore, new compositions were formulated incorporating an additional flux. 10 wt% Na_2O (as Na_2CO_3 of A.R. quality) was selected since at low percentages alkaline oxides act as a fluxes, lowering the melting temperature of the glass (Sheng 2001). Furthermore, due to its role as glassy network modifier, the Na_2O decreases the melt viscosity, thereby facilitating the casting step (Fernández Navarro, 2003). Therefore, the compositions CEC703010 (63.8% fly ash, 27.0% metallurgical slag, 10.0% Na_2O) and CEC653510 (58.5% fly ash, 31.5% metallurgical slag, 10.0% Na_2O) were tested and whereas the CEC703010 composition resulted in an unworkable, high viscosity melt, the CEC653510 composition led to a workable, low viscosity melt. In view of these results, the CEC653510 mixture was selected for the recovery of fly ash and metallurgical slag. After melting and pouring, the CEC653510 composition results in a homogeneous glass with glossy dark green colour. Hereinafter this glass will be designated as CEC glass.

Figure 6 shows the diffractogram recorded from the CEC glass sample, a broad diffraction halo in the 2θ = 20-40° range is characteristic of amorphous materials. The absence of defined diffraction peaks indicating the occurrence of crystalline phases indicates that during the melting process the different crystalline phases contained in the raw materials experimented multiple modification including crystalline transformations, reactions between different chemical species, melting and dissolution in the forming melt. As result, a homogeneous glass is obtained after melt cooling.

Table 4 show the chemical composition determined by XRF. Tables 5 and 6 collect the results of the equilibrium leaching tests L/S 2 and L/S 10 (UNE EN 12457-1 and 2) respectively together with the leaching limits values established by the Council of the European Union for waste classification.

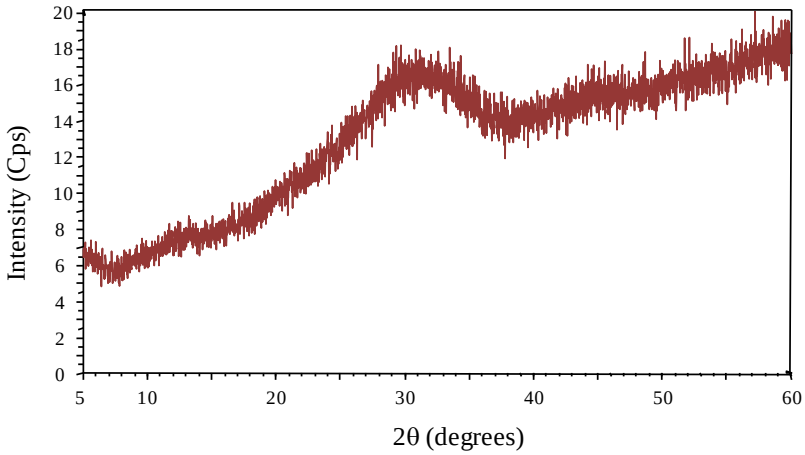

Fig. 6 X-ray diffraction pattern of CEC glass

Table 4. XRF analysis (wt %) of the original CEC glass.

SiO_2	Al_2O_3	Fe_2O_3	MgO	CaO	Na_2O	K_2O	MnO	SO_3	P_2O_5	TiO_2
42.88	18.10	4.98	4.94	14.12	11.60	0.83	0.84	0.28	0.23	0.97

The measured values of pH and conductivity indicate that the CEC glass developed from Petacalco fly ash and Arcelor Mittal slag shows higher chemical stability than the starting wastes. Thus, the conductivity of the leachates derived from the CEC glass is one magnitude order lower than those measured over the leachates collected from both fly ash and slag. The lower concentration of extracted ions indicates that vitrification leads to a stabilization process in which the inorganic components of the wastes are immobilized by incorporating them into the glass structure.

Concerning the pH, the chemical attack of a glass by pure water is an ion exchange process that begins with the penetration of a proton from water into the glassy network, replacing an alkali ion into solution (Paul 1990):

$\equiv Si\text{-}O^{-}R^{+} + H^{+} + OH^{-} \rightarrow \equiv Si\text{-}OH + Na^{+}OH^{-}$

Table 5. Concentration (mg kg^{-1} dry substance) of elements in the leachates according to the equilibrium leaching test L/S 2 (UNE EN 12457-1) and leaching limit values for waste classification.

	Fly ash	**Slag**	**Glass**	**Inert waste**	**Non-hazardous waste**	**Hazardous waste**
pH	12.15	12.35	10.79	___	___	___
Conductivity ($mScm^{-1}$)	2.21	3.08	0.69	___	___	___
As	<dl	<dl	<dl	0.1	0.4	6
Ba	0.21	1.79	0.04	7	30	100
Cd	<dl	<dl	<dl	0.03	0.6	3
Cr total	0.53	0.02	0.25	0.2	4	25
Cu	<dl	<dl	0.42	0.9	25	50
Hg	0.42	14,745	0.048	0.003	0.05	0.5
Mo	5.06	<dl	0.03	0.3	5	20
Ni	<dl	<dl	0.15	0.2	5	20
Pb	<dl	<dl	<dl	0.2	5	25
Sb	<dl	<dl	<dl	0.02	0.2	2
Se	<dl	<dl	<dl	0.06	0.3	4
Zn	<dl	<dl	<dl	2	25	90
Chloride	5.88	44.36	9.28	550	10000	17000
Fluoride	9.48	21.61	10.01	4	60	200
Sulphate	942.06	8.76	22.12	560	10000	25000

The diffusion of protons into the glass determines the removal of Na^{+} ions and the formation of OH^{-} groups in the aqueous medium. If the dissolution is not renewed and remains stationary in contact with the glass such as in the leaching test, the pH of the solution is getting higher and the leachate is becoming more aggressive, initiating the dissolution of the glass network. The pH of the leachates

derived from CEC glass is lower than those for the leachates obtained from both fly ash and slag, indicating again that vitrification results in the stabilization of the ions within the glassy network.

Table 6. Concentration (mg kg^{-1} dry substance) of elements in the leachates according to the equilibrium leaching test L/S 10 (UNE EN 12457-2) and leaching limit values for waste classification.

	Fly ash	**Slag**	**Glass**	**Inert waste**	**Non-hazardous waste**	**Hazardous waste**
pH	11.75	12.92	9.46	___	___	___
Conductivity ($mScm^{-1}$)	1.05	1.95	0.23	___	___	___
As	<dl	<dl	<dl	0.5	2	25
Ba	2.66	0.94	0.21	20	100	300
Cd	<dl	<dl	<dl	0.04	1	5
Cr total	0.61	<dl	0.09	0.5	10	70
Cu	<dl	0.04	0.13	2	50	100
Hg	4.58	2.801	0.19	0.01	0.2	2
Mo	3.81	<dl	<dl	0.5	10	30
Ni	<dl	<dl	<dl	0.4	10	40
Pb	<dl	<dl	<dl	0.5	10	50
Sb	<dl	<dl	<dl	0.06	0.7	5
Se	<dl	<dl	<dl	0.1	0.5	70
Zn	<dl	<dl	<dl	4	50	200
Chloride	0	26.73	131.12	800	15000	25000
Fluoride	21.26	44.31	21.66	10	150	500
Sulphate	1,755.47	560.60	21.05	1000	20000	50000

With regard to the concentration of extracted elements in the leachates, the equilibrium leaching test L/S 2 (Table VI) shows that both Petacalco fly ash and Arcelor Mittal slag exceed the limits of Hg and Mo established by the Annex II to Directive 1999/31/EC for wastes acceptable at landfills for non-hazardous wastes and consequently, they must be deposited in special landfills for hazardous wastes. As above mentioned the vitrification of those wastes causes the partial immobilization of

metals and reduces their concentration in the leachates to acceptable limits so that CEC glass can be considered as non-hazardous. Similar result is found with the equilibrium leaching test L/S 10 (Table VII). In this case, according the concentration of Hg in the leachates derived from Petacalco fly ash and Arcelor Mittal slag, those waste are classified as wastes to be deposited in landfills for hazardous wastes. Therefore, the mobility of Hg decreases in CEC glass produced from a mixture of these wastes and CEC glass can be considered as non-hazardous.

Therefore, the vitrification of Petacalco fly ash and Arcelor Mittal slag results in a durable glass showing good behaviour in the leaching tests. Moreover, vitrification reduces the volume of waste material. However, the major limitation is that vitrification requires large amounts of energy to process wastes and, thus, may be more expensive compared to other remedial technologies. As explained below, the last goal of this study is to valorise the wastes as crystallised glass tiles suitable for floor pavement and wall recovering. With this aim, the most suitable way to obtain the glass is by melting raw materials and subsequent quenching of the melt in water, thus transformed the melt into a solid, insoluble, fragmented glass (frit). Frits furnaces are usually smaller than other furnaces in the glass industry (< 20 tonnes per day). All existing frit furnaces are natural gas-fired, and the energy required per tonne of melted frits is similar to other glass sectors (above 13GJ/tonne, corresponding to 300 Nm^3 of gas per tonne of frit) (Scalet et al. 2013). One way to increase the competitiveness of the process would be get glasses with specific applications. In this sense, this research is part of a larger study that explores the possibility of valorising Mexican coal fly ash as glass-ceramic (crystallised glass) tiles suitable for floor pavement and wall recovering. For a preliminary knowledge of technological features of these materials, CEC glass was subjected to a thermal treatment at 1100ºC/5 and the resulting glass-ceramic material was tested in order to determine its water absorption (0.02%) and bending strength (71 N/mm^2) values. With these properties, the developed glass-ceramic are within BIa group of the standard ISO 13006 and are suitable for floor pavement and wall covering in both indoor and outdoor applications.

Conclusion

This study investigates the characterisation of a Mexican coal fly ash and a metallurgical slag and their valorisation through a vitrification process. The Petacalco fly ash consists of α-quartz (SiO_2), hematite (Fe_2O_3) and mullite ($Al_6Si_2O_{13}$) together with a significant amount of amorphous phase.

The characterisation results indicate that it likely will show a highly refractory behaviour in a melting process. The findings supporting this assumption are as follows: It is a type F fly ash with high SiO_2 + Al_2O_3 percentage (about 76 wt. %); The particle size is too fine, with about 90% of the sample with particle size lower than 100 µm; The DSC curve does not show endothermic peaks indicative of the formation of liquid phases at high temperature.

The Arcelor Mittal metallurgical slag shows low content (~25 wt. %) in network forming elements and high percentage in alkaline and alkaline-earth elements (~60 wt. %). Moreover, its DSC curve shows liquid phases formation at 1080ºC. These features became this metallurgical slag useful as complementary raw material for formulating glass compositions.

The vitrification study shows that the optimum composition to maximise use of Petacalco fly ash, while producing a melt with an acceptable viscosity is 58.5 wt% fly ash + 31.5 wt% Arcelor Mittal metallurgical slag + 10.0 wt% Na_2O (designated CEC).

Equilibrium leaching test show that the conductivity and pH in the leachates derived from CEC glass is lower than those measured over the leachates collected from both fly ash and slag, which indicates that vitrification leads to a stabilization process in which the inorganic components of the wastes are immobilized by incorporating them into the glass structure.

With regard to the concentration of extracted elements in the leachates, Petacalco fly ash and Arcelor Mittal slag are classified as wastes to be deposited in landfills for hazardous wastes whereas CEC glass can be considered as non-hazardous. Moreover, a preliminary study showed that CEC glass is suitable for developing glass-ceramic tiles appropriate for floor pavement and wall covering.

Acknowledgements

The authors thank Mrs. P. Díaz and Mrs. E. Sánchez for their technical assistance. H. R. Guzmán-Carrillo wants to thank CONACyT for scholarship (Grant nº 311363) and to Prof. J. Ma. Rincón from the IETcc-CSIC for his valuable advice.

References

1. Eliche-Quesada D, Leite-Costa J (2016) Use of bottom ash from olive pomace combustion in the production of eco-friendly fired clay bricks. Waste Manage 48:323-333. doi: 10.1016/j.wasman.2015.11.042
2. Erol M, Genç A, Öveçoğlu ML, Yücelen E, Küçükbayrak S, Taptik Y (2000) Characterization of a glass-ceramic produced from thermal power plant fly ashes. J Eur Ceram Soc 20:2209–2214. doi:10.1016/S0955-2219(00)00099-6
3. Faleschini F, Zanini MA, Brunelli K, Pellegrino C (2015) Valorization of co-combustion fly ash in concrete production. Mater Design 85:687-694. doi:101016/jmatdes201507079
4. Fernández Navarro JM (2003) El Vidrio, third ed, Editorial SCIC, Madrid
5. Fomenko EV, Anshits NN, Solovyov LA, Mikhaylova OA, Anshits AG (2013) Composition and morphology of fly ash cenospheres produced from the combustion of Kuznetsk coal. Energ Fuels 27:5440–5448. doi: 101021/ef400754c
6. Gallardo M Almanza, JM, Cortés DA, Escobedo JC, Escalante-García J (2014) Synthesis and mechanical properties of a calcium sulphoaluminate cement made of industrial wastes. Mater Construcc 64:e023. doi:103989/mc201404513
7. Iyer S, Scott JA (2001) Power station fly ash-a review of value-added utilization outside of the construction industry Resour Conserv Recy 31:217–228 doi:101016/S0921-3449(00)00084-7
8. Jarosz-Krzeminska E, Helios-Rybicka E, Gawlicki M (2015) Utilization of neutralized spent sulfuric acid pickle liquor from metal treatment in cement production. Int J Environ Sci Technol 12:2901-2908. doi: 10.1007/s13762-014-0694-9
9. Jayaranjan MLD, Van Hullebusch ED, Annachhatre AP (2014) Reuse options for coal fired power plant bottom ash and fly ash Rev Environ Sci Bio 13:467-486 doi:101007/s11157-014-9336-4
10. Karamanov A, Chabbach LM, Karamanova E, Andreola F, Barbieri L, Ranguelov B, Avdeev G, Lancellotti I (2014) Sinter-crystallization in air and inert atmospheres of a glass from pre-treated municipal solid waste bottom ashes. J Non-Cryst Solids 389:50-59. doi: 101016/jjoncrysol201402009
11. Kim JM, Kim HS (2004) Processing and properties of a glass-ceramic from coal fly ash from a thermal power plant through an economic process. J Eur Ceram Soc 24:2825–2833. doi:101016/jjeurceramsoc200308012
12. Ljatifi E, Kamusheva A, Grozdanov A, Paunovic P, Karamanov A (2015) Optimal thermal cycle for production of glass-ceramic based on wastes from ferronickel manufacture. Ceram Int 41:11379-11386. doi: 101016/jceramint201505098
13. López O, Mayor PL, Fernández F, Hernandez-Olivares F (2015) Improved cement mortars by addition of carbonated fly ash from solid waste incinerators. Mater Construcc 65:e062. doi:103989/mc201507114

14. Martínez-Martínez S, Pérez-Villarejo L, Eliche-Quesada D, Carrasco-Hurtado B, Sánchez-Soto PJ, Angelopoulos GN (2016) Ceramics from clays and by-product from biodiesel production: Processing, properties and microstructural characterization. Appl Clay Sci 121:119-126. doi: 101016/jday201512003
15. M. Romero, M. Kovacova, J. Ma. Rincón (2008) Effect of particle size on kinetics crystallization of an iron-rich glass. J Mater Sci 43:4135-4142. doi: 10.1007/s10853-007-2318-y
16. Pan DA, Li LJ, Yang J, Bu JB, Guo B, Liu B, Zhang SG, Volinsky AA (2015) Production of glass-ceramics from heavy metal gypsum and pickling sludge. Int J Environ Sci Technol 12:3047-3052. doi:10.1007/s13762-015-0758-5.
17. Pani GK, Rath P, Maharana L, Barik R, Senapati PK (2016) Assessment of heavy metals and rheological characteristics of coal ash samples in presence of some selective additives. Int J Environ Sci Technol 13:25-731 doi: 101007/s13762-015-0888-9
18. Paul A (1990) Chemistry of Glasses, 2nd ed, Chapman ad Hall, New York
19. Pérez M, Baeza F, Paya J, Saval JM, Zornoza E, Borrachero MV, Garces P (2014) Potential use of sewage sludge ash (SSA) as a cement replacement in precast concrete blocks. Mater Construcc 64:e002. doi:103989/mc201406312
20. Ram LC, Masto RE (2010) An appraisal of the potential use of fly ash for reclaiming coal mine spoil. J Environ Manag 91:603–617. doi:101016/jjenvman200910004
21. Ram LC, Masto RE (2014) Fly ash for soil amelioration: a review on the influence of ash blending with inorganic and organic amendments. Earth-Sci Rev 128: 52–74. doi:101016/jearscirev201310003
22. Reuter M, Xiao Y, Boin U (2004) Recycling and environmental issues of metallurgical slags and salt fluxes. In: II International Conference on Molten Slags Fluxes and Salts. The South African Institute of Mining and Metallurgy, pp 349-356
23. Rodríguez Cuartas R (1984) Theoretical calculation of glass properties: viscosity, thermal and devitrification parameters (in Spanish). Bol Soc Esp Ceram Vidr 23:105-111
24. Saikia N, Mertens G, Van Balen K, Elsen J, Van Gerven T, Vandecasteele C (2015) Pre-treatment of municipal solid waste incineration (MSWI) bottom ash for utilisation in cement mortar. Constr Build Mater 96:76-85. doi:101016/jconbuildmat201507185
25. Scalet BM, Garcia Muñoz M, Sissa AQ, Roudier S, Delgado Sancho L (20013). Best Available Techniques (BAT) Reference Document for the Manufacture of Glass. Industrial Emissions Directive 2010/75/EU Integrated Pollution Prevention and Control
26. Sharma P, Joshi H (2016) Utilization of electrocoagulation-treated spent wash sludge in making building blocks. Int J Environ Sci Technol 13: 349-358. doi: 10.1007/s13762-015-0845-7

27. Seyyedalipour SF, Kebria DY, Dehestani M (2015) Effects of recycled paperboard mill wastes on the properties of non-load-bearing concrete. Int J Environ Sci Technol 12:3627-3634. doi: 10.1007/s13762-015-0879-x
28. Sheng J (2001) Vitrification of borate waste from nuclear power plant using coal fly ash (I) glass formulation development. Fuel 80:1365-1369. doi:101016/S0016-2361(01)00022-9
29. Skousen J, Ziemkiewicz ZP, Yang JE (2012) Use of coal combustion by-products in mine reclamation: review of case studies in the USA. Geosyst Eng 15:71–83. doi:101080/122693282012676258
30. Verbinnen B, Block C, Van Caneghem J, Vandecasteele C (2015) Recycling of spent adsorbents for oxyanions and heavy metal ions in the production of ceramics. Waste Manage 45:407-411. doi:101016/jwasman201507006
31. Wang SM, Zhang CX, Chen JD (2014) Utilization of coal fly ash for the production of glass-ceramics with unique performances: A brief review. J Mater Sci Technol 30:1208-1212. doi:101016/jjmst201410005
32. Wee JH (2013) A review on carbon dioxide capture and storage technology using coal fly ash. Appl Energy 106:143–151. doi:101016/japenergy201301062
33. Yao ZT, Ji XS, Sarker PK, Tang JH, Ge LQ, Xia MS, Xi YQ (2015) A comprehensive review on the applications of coal fly ash Earth Sci Rev 141: 105–121 doi:101016/jearscirev201411016
34. Zheng YJ, Jensen AD, Windelin J, Jensen F (2012) Review of technologies for mercury removal from flue gas from cement production processes. Prog Energy Combust Sci 38:599–629. doi:101016/jpecs201205001